Relationship of Salt Marsh Vegetation Zonation to Spatial Patterns in Soil Moisture, Salinity, and Topography

Kevan B. Moffett,[1]* David A. Robinson,[2] and Steven M. Gorelick[1]

[1]Department of Environmental Earth System Science, Stanford University, Stanford, California 94305, USA; [2]Centre for Ecology and Hydrology, Environment Centre Wales, Bangor, Gwynedd LL57 2UW, UK

ABSTRACT

An intertidal San Francisco Bay salt marsh was used to study the spatial relationships between vegetation patterns and hydrologic and edaphic variables. Multiple abiotic variables were represented by six metrics: elevation, distance to major tidal channels and to the nearest channel of any size, edaphic conditions during dry and wet circumstances, and the magnitude of tidally induced changes in soil saturation and salinity. A new approach, quantitative differential electromagnetic induction (Q-DEMI), was developed to obtain the last metric. The approach converts the difference in soil electrical conductivity (ECa) between dry and wet conditions to quantitative maps of tidally induced changes in root zone soil water content and salinity. The result is a spatially exhaustive map of edaphic changes throughout the mapped area of the ecosystem. Spatially distributed data on the six metrics were used to explore two hypotheses: (1) multiple abiotic variables relevant to vegetation zonation each exhibit different, uncorrelated, spatial patterns throughout an intertidal salt marsh; (2) vegetation zones and habitats of individual plant species are uniquely characterized by different combinations of key metrics. The first hypothesis was supported by observed, uncorrelated spatial variability in the metrics. The second hypothesis was supported by binary logistic regression models that identified key vegetation zone and species habitat characteristics from among the six metrics. Based on results from 108 models, the Q-DEMI map of saturation and salinity change was the most useful metric of those tested for distinguishing different vegetation zones and plant species habitats in the salt marsh.

Key words: pattern; salt marsh; vegetation; zonation; edaphic; wetland; geophysics; ECa; Q-DEMI.

INTRODUCTION

The segregation of a few dominant plant species into distinctive zones is characteristic of intertidal salt marshes. Each zone comprises a distinctive macrophyte assemblage and may also uniquely sustain other species of concern. For example, stands of native *Spartina foliosa* densely dissected by tidal channels in San Francisco Bay support endangered

Rallus longirostris obsoletus (California Clapper Rails), but endangered *Reithrodontomys raviventris* (Salt Marsh Harvest Mice) favor largely monospecific and undissected *Salicornia virginica* flats (USFW 2008). The nature and causes of this ecologically important vegetation zonation have been studied for decades with gradient analyses and paired plot, mesocsosm, or transplant studies. Such studies have determined that the causes of salt marsh vegetation zonation are both physical, determined in part by variability in soil (edaphic) and tidal conditions (Pennings and others 2005), and biological, the result of interspecific resource competition and biological response to periodic disturbance (Bertness and others 1992; Emery and others 2001; Pennings and Callaway 1992), even as the specific patterns and species vary regionally (Peterson and others 2008).

At the ecosystem scale, it remains a challenge to explain salt marsh vegetation patterning despite knowledge of specific zonation mechanisms at the plant scale. Characterization of the spatial variability of vegetation within salt marsh ecosystems has thus far relied heavily on metrics of relative landscape position such as elevation and distance to tidal channels; however, these geographic metrics, alone, have been insufficient predictors of salt marsh vegetation zones (Zedler and others 1999; Silvestri and others 2005). Although remote sensing has been used to map spatial patterns of tidal channels (for example, Marani and others 2006) and marsh surface elevations (for example, Sadro and others 2007) in relation to salt marsh vegetation, such maps fail to distinguish unique and consistent salt marsh vegetation habitat characteristics. Probabilistic models based on geographic metrics (for example, Sanderson and others 2001) fare somewhat better, but the fraction of marsh vegetation cover predicted correctly is greatly skewed by very high or very low coverage by a given species. Part of the difficulty in such analyses is that geographic metrics are only rough proxies for the combined effects of many physical, chemical, and biological variables that contribute to salt marsh zonation.

In this study, we explored two hypotheses about the spatial nature of zonation-relevant variables and their relationship to salt marsh vegetation distribution. First, we hypothesized that different variables, such as tidal flood duration and direction, root zone soil water content, and soil salinity, each exhibit different spatial patterns in a salt marsh. The patterns of such variables may have different characteristic spatial scales and gradients oriented in opposing directions. Second, we hypothesized that each plant species and zone correlates with different combinations of variables. For example, one species might grow among dry soil conditions or high soil salinity, but not both; another species might not grow among dry or salty edaphic conditions. Also, due to interspecific interactions, a zone dominated by one species may not be characterized by the same variables as the total habitat range of the species. This study tested such concepts in a spatially distributed manner throughout an intertidal salt marsh on the basis of extensive data sets spanning the full range of conditions within the marsh.

We examined the first hypothesis by comparing the spatial patterns of six zonation-relevant metrics: (1) elevation, (2) distance to major tidal channels and (3) to the nearest channel of any size, (4) the soil saturation/salinity state during dry and (5) wet marsh conditions, and (6) the difference in this edaphic state between wet and dry conditions. The first three metrics are geographic measures of landscape position and proxies for hydrologic processes relevant to salt marsh vegetation zonation. Elevation is commonly employed to represent the effects of flood/exposure duration and surface water ponding. A location's distance to the nearest tidal channel represents the likely direction of tidal flooding, groundwater drainage, and directional tidal energy effects (for example, sediment deposition). This study considered both distances to primary tidal channels, typically identified from aerial imagery, and distances to small permanent surface drainage pathways hidden beneath the vegetation that we term microtributaries.

The remaining three metrics described soil properties under different hydrologic conditions (dry and wet marsh soils) and the magnitude of change between conditions. The soil properties considered, soil saturation, salinity, and texture, are known to contribute to salt marsh zonation (Silvestri and others 2005) but previously could only be measured at points, prohibiting extensive repeat sampling and marsh-wide analysis. Geophysical electromagnetic induction (EMI) imaging of bulk apparent soil electrical conductivity (ECa) captures the combined state of soil saturation, salinity, and texture in one ECa number (Friedman 2005; Rhoades and others 1999) and can be surveyed quickly over a large area. EMI has been used to investigate patterns in soil properties (for example, Scanlon and others 1999; Lesch and others 2005; Robinson and others 2009) but its potential to provide new insight into ecosystem patterning is only beginning to be explored (Stroh and others 2001; Paine and others 2004; Robinson and others 2008a). Prior to this study the method

had not been tested in an environment with as extremely high soil water, salt, and clay contents as in salt marshes with the possible exception of some of the transects by Paine and others (2004). To further the applicability of EMI to salt marsh vegetation analysis, we developed a method to filter out the effects of the soil clay content on the ECa data and leverage the information on changes in soil saturation and salinity from sequential EMI surveys from different hydrologic conditions. Our approach was to subtract the data from two EMI surveys (differential or time-lapse EMI; Lesch and others 2005; Robinson and others 2009) and then convert the ECa difference values (ΔECa) to quantitative estimates of soil water content and salinity change using Archie's Law (quantitative differential EMI, or Q-DEMI). Our Q-DEMI methodology quantified tidally induced saturation and salinity changes in the salt marsh root zone and enabled assessment of their spatial relationship to vegetation zonation throughout a marsh in unprecedented detail.

To explore the second hypothesis, that each salt marsh plant species might bear a different relationship to a suite of relevant variables, we sought to isolate distinguishing characteristics of each of the major vegetation zones and individual plant species habitats composing the salt marsh ecosystem. We used logistic regression modeling to assess the correlation between vegetation patterns and the six geographic and edaphic metrics. The geophysical data on salt marsh edaphic conditions provided greater insight into the underlying abiotic characteristics of the vegetation patterns than was gained from the geographic metrics alone. In particular, spatial variability in tidally induced changes in soil water content and salinity reflected in the Q-DEMI ΔECa metric was the most effective means of distinguishing vegetation zones and habitats.

Multiple variables combine to support ecosystem structures, functions, habitat heterogeneity, integrity, and supply of ecosystem services of salt marshes (Turner and Chapin 2005; Peterson and others 2008), but these variables are seldom analyzed in a spatially distributed manner. With this study we aimed to better understand how the effects of multiple abiotic variables combine to produce an emergent pattern, a spatially variable abiotic template upon which salt marsh vegetation patterns and biotic interactions are expressed. A system-level perspective that integrates both abiotic and biotic variables may help inform the maintenance and restoration of coastal wetlands, a matter of increasing interest worldwide amid concerns of sea

level rise, increased storm activity, and coastal development pressure (Peterson and others 2008).

MATERIALS AND METHODS

Field Site and Hydrology

The study site was a 0.9 ha intertidal salt marsh in southern San Francisco Bay, within the Palo Alto Baylands Nature Preserve (37°27′54″N, 122°6′58″W) (Figure 1). The geological and botanical history of the surrounding Santa Clara Valley were described by Cooper (1926) and the geology underlying the Palo Alto Baylands by Hamlin (1983). The history and character of the marsh were similar to that described by Hinde (1954) for the adjacent marsh to the south. We employed this site as a model for exploring western North America salt marsh vegetation patterning and the utility of portable EMI
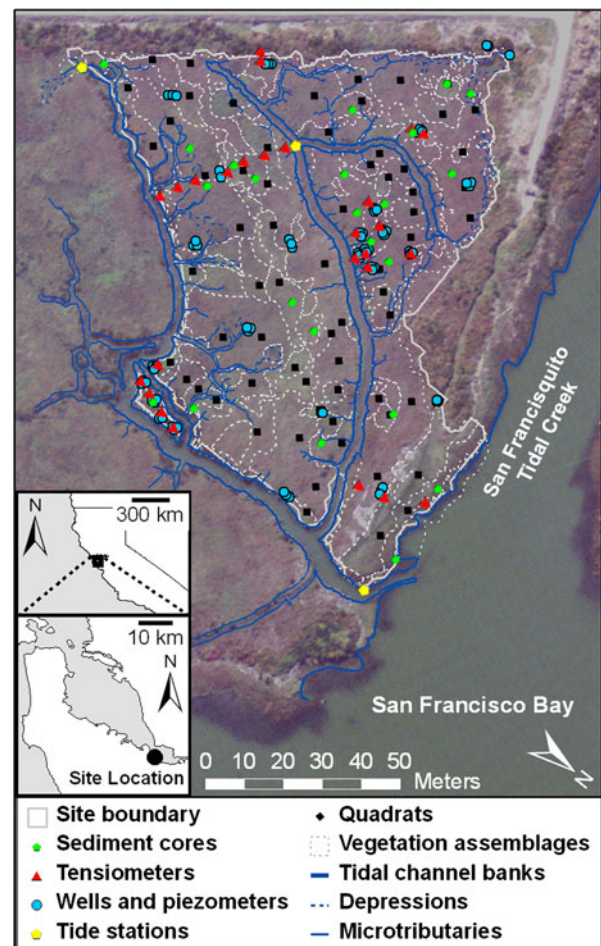

Figure 1. Field site location, site map, and spatial distribution of sampling locations.

methods for better understanding abiotic coastal ecosystem patterns. The underlying site stratigraphy consisted of 3–5 m of fine estuarine mud, predominantly montmorillonite clay, overlying a saline aquifer system (Hamlin 1983).

Vegetation Mapping

Plant species at the site were: *Spartina foliosa*, *Salicornia depressa* (*S. virginica*), *Distichlis spicata*, *Jaumea carnosa*, *Grindelia stricta*, *Frankenia salina*, *Salsola soda*, and *Atriplex prostrata* (see USDA (2009) for synonymous species names). The habitat occupied by each species was mapped by marking the boundaries of assemblages distinguished by the presence/absence of each of the species, digitizing these polygonal boundaries using streaming GPS, and identifying the relative abundance of each species within each polygon. This method was similar to that of Zedler and others (1999) for San Diego Bay marshes, but with greater emphasis on identifying the locations of assemblage boundaries. Surveys of species' percent cover within 1-m^2 quadrats verified assemblage composition at 69 locations. The 57/134 assemblage polygons verified by one or more quadrats accounted for 81% of the marsh area. The remaining 19% of marsh area was covered by 77 smaller polygons. Figure 1 shows the digitized assemblage polygons and quadrat locations, illustrating the means by which a limited number of quadrat-containing polygons represented most of the marsh area.

Vegetation zones were classified by the species of greatest (dominant) cover fraction in each assemblage polygon. The quadrat surveys confirmed that this was a sufficient means of identifying vegetation zones because assemblage composition within each zone defined in this manner was consistent. In addition to the spatial distribution of major vegetation zones, in this study we were interested in the full range of conditions among which each plant species grew. We refer to a plant species' habitat as all the areas the species occupied regardless of cover density. In our vegetation discrimination analysis we assessed the salient characteristics of zones and species habitats separately and compared the results.

Mapping Edaphic Conditions

A logical precursor to understanding salt marsh vegetation distribution is a thorough description of root zone edaphic conditions throughout the ecosystem, but obtaining spatially extensive data on relevant physical and chemical soil properties has been intractable with point-sampling methods. The combination of heterogeneous soil water content, salinity, and clay fraction was captured in this study by the parameter bulk soil electrical conductivity (ECa). The ECa data were mapped on 2 separate days by repeatedly traversing the field site carrying a streaming EMI instrument (DUALEM-1S, Dualem, Inc., Milton, Ontario, Canada) and GPS, logged concurrently. Sequential traverses were separated to account for the approximately 4 m^2 EMI measurement support area. We estimated the vertical soil interval represented by the ECa data was 0–0.40 m depth (see online supplement for calculations), approximately the depth of the salt marsh root zone. We post-processed approximately 5000 ECa measurements per survey (Robinson and others 2008a) and corrected for effects of soil temperature (Reedy and Scanlon 2003) to produce kriged ECa maps at 2-m resolution. EMI instrument accuracy was 0.001 dS/m. Successive measurements of ECa at multiple test locations agreed to within 0.01 dS/m, which we take to be the ECa uncertainty in this study. The value of 0.01 dS/m was the 95% confidence level for the mean of a streaming series of 1479 consecutive ECa measurements collected at a stationary point. Calculation of the median difference between ECa measurements from 5859 pairs of nearly identical locations measured at different times resulted in a second estimate of 0.015 dS/m; due to its greater uncertainty, the second method was used only as a rough check on the result from the first method (see supplement for details). We took precautions in the field to reduce measurement uncertainty: conducting all surveys using the same person, holding the instrument from a fixed strap with a vertical, stiff arm, and surveying over extremely flat terrain. Uncertainty from even 20 cm of height offset (highly unlikely) would still be comparable to our stated uncertainty magnitude (Abdu and others 2007).

The two EMI surveys were timed to capture different hydrologic conditions. The first survey occurred just prior to the neap–spring tidal transition, when the marsh had not been flooded in 8 days (Nov. 19, 2007); we refer to these as data from ''dry'' marsh conditions. The second survey was partially into the next spring tide cycle, immediately following a flood tide (Dec. 7); we refer to these as data from ''wet'' marsh conditions. We use the terms ''dry'' and ''wet'' as qualitatively convenient reminders of antecedent tidal conditions although both circumstances represent very moist soils (>80% saturation). Both survey times were near mid-day and no rain occurred while the

marsh surface was exposed during the study period.

The field site experiences mixed semi-diurnal tides and a semi-arid Mediterranean climate with winter precipitation ($\sim$39 cm y^{-1}). The marsh plain is above mean high water and is flooded by the higher high tide on 2/3–3/4 of days during each spring–neap cycle with the variability in flood frequency due to the nature of the mixed semi-diurnal tides. To verify ambient hydrologic conditions, we monitored groundwater and tidal conditions at the site by logging pressure and temperature every 10 min at the bed of the two primary tidal channels and in 43 wells and piezometers (Freeze and Cherry 1979) installed 0.5–1.0 m into the marsh substrate (Figure 1). We monitored hydraulic heads in the root zone with 23 tensiometer pairs (Freeze and Cherry 1979) spanning 10–15 and 20–25 cm depths (Figure 1). Tensiometer data were collected manually during the geophysical surveys.

Empirical relationships have shown ECa to increase with increasing soil clay content, water content (θ), or solution electrical conductivity (ECw) (for example, Rhoades and others 1999), though not for values as high as those that occur in salt marshes. We conducted laboratory analyses to establish the specific relationships between ECa and salt marsh soil properties. Twenty-three soil sampling locations were strategically chosen using the ECa data from the first survey and response-surface directed sampling (Corwin and Lesch 2005; Lesch 2005) (Figure 1). After collecting ECa data at each location, soil cores (2.5 cm diameter) were collected manually from 0–30 cm and 30–60 cm depths. The 0–30 cm depth interval was chosen to correspond roughly to the EMI signal depth, enabling correlation with ECa survey data. The 30–60 cm deep samples were used in parameterizing the Q-DEMI methodology, discussed below. The cores were immediately sealed in plastic bags and promptly weighed in the laboratory. Samples were air-dried for 11–28 days, homogenized subsamples weighed, oven-dried at 105°C for at least 12 h and re-weighed, and core water fractions and bulk densities calculated. Duplicate homogenized subsamples were analyzed for soil paste extract electrical conductivity (ECe) and soil texture (University of Idaho Pedology Laboratory standard procedures). Pore water samples extracted adjacent to the coring locations from 30 cm depth using a suction lysimeter ("sipper", $\sim \leq 5$ kPa suction; Roman and others 2001) were analyzed in the laboratory for pore water electrical conductivity (ECw).

Quantitative Differential EMI Methodology

Each geophysical survey provided a snapshot of the combination of water, salt, and clay conditions throughout the salt marsh at one point in time. We developed a method to transform the difference in ECa between dry and wet tidal conditions into spatially distributed, quantitative estimates of changes in root zone soil water content and salinity. The premise of the Q-DEMI method was that a change in the ECa value of a location was due to changing soil water content and salinity while clay content remained constant. In our Q-DEMI analysis, we subtracted the later "wet" ECa data from the earlier "dry" ECa data, simulating a case of increasing soil moisture (ΔECa = ECa$_{dry}$ − ECa$_{wet}$). We then determined the nature of the edaphic change, whether caused by changing soil water content or by changing soil salinity, from the sign of ΔECa. An observed increase in ECa between dry and wet conditions ($-\Delta$ECa) indicated an increase in soil water content: an increase in salt content could not explain the change in these areas because tidal waters were known a priori to be less saline (EC$_{tide}$ = 33.4 dS/m) than the marsh pore waters (ECw = 57.2 dS/m) to which they were added to wet-up the marsh. In contrast, an observed decrease in ECa ($+\Delta$ECa) indicated a decrease in pore water salinity: under conditions of increasing tidal water availability, water content would remain constant or increase and so could not explain the ECa change in these areas. Because saturation and salinity changes could occur simultaneously with opposing effects, the Q-DEMI calculations represent the conservative case in which all ECa change is ascribed to the dominant process identified by the sign of ΔECa.

Quantifying saturation and salinity changes was accomplished using Archie's Law. Archie's Law is a well-studied empirical petrophysical relationship between ECa and: pore water conductivity (ECw), a formation factor (f) related to porosity, the soil saturation (S), and the soil mineral surface conductivity due to adsorbed ionic charge (σ_s) (Kirsch 2006).

$$ECa = ECw \cdot f \cdot S^2 + \sigma_s \qquad (1)$$

The mineral surface conductivity (σ_s) is important in soils with large clay fractions, such as in our salt marsh, but has not been tabulated for salt marsh clay soils. We estimated f and σ_s using a simple linear regression between ECa and pore water conductivity (ECw) for saturated samples ($S = 1$). The soil samples used for this regression

were from 30–60 cm depth because these samples were known to be from the saturated zone below the water table. The resulting f and σ_s parameter estimates compared favorably with estimates from more complicated methods (see online supplement). These parameters permitted Q-DEMI calculation of changes in saturation, due to aerated pore space being filled by tidal waters, and changes in salinity, due to flushing of salt marsh soils, using variations on Archie's Law.

In the saturation-change dominated ($-\Delta$ECa) areas of the marsh we solved Archie's Law (equation (1)) for the net soil water content change required to account for the observed increase in ECa between dry and wet marsh conditions. To reduce one excess degree of freedom in the calculation we assumed that initially aerated pore space in the soil was completely filled by the flood tide, leading to a minimum estimate of soil saturation change because the effect of any trapped air would have reduced the magnitude of ΔECa. The formula we derived to calculate saturation change (ΔS) is shown below (equation (2)). The parameters are the: formation factor (f), mineral surface conductivity (σ_s), tidal flood water electrical conductivity (EC_{tide}), and measured ECa during wet (ECa_{wet}) and dry (ECa_{dry}) conditions.

saturated throughout dry and wet marsh conditions through the combination of the shallow water table and large capillary rise in the fine sediments.

In addition to the two maps of ECa, from dry and wet marsh conditions, the map of saturation and salinity changes produced by the Q-DEMI methodology provided a third spatially distributed metric of salt marsh root zone characteristics against which to compare salt marsh vegetation zonation. Estimating the spatial distribution of soil saturation changes for these systems is an advance in itself, as dielectric soil moisture sensors will not work in the saline environment (Robinson and others 2008b), resulting in destructive sampling being the only other option.

Mapping Marsh Geometry

Geometric measures of spatial context within the ecosystem have traditionally been employed as indicators of salt marsh ecosystem structure and spatially variable intertidal hydrologic effects. The most common such geographic, or "landscape position" (Zedler and others 1999), metrics are elevation and distance-to-channel. We mapped these metrics at the same high resolution as our edaphic

$$\Delta S = \frac{-(\sigma_s - ECa_{wet} - f \cdot EC_{tide}) - \sqrt{(\sigma_s - ECa_{wet} - f \cdot EC_{tide})^2 - 4 \cdot (f \cdot EC_{tide}) \cdot (ECa_{wet} - ECa_{dry})}}{2 \cdot (f \cdot EC_{tide})} \quad (2)$$

The real solution to equation (2) using a positive discriminant root yielded unrealistic ΔS values greater-than one, so was discarded.

In the salinity-change dominated ($+\Delta$ECa) areas of the marsh we solved Archie's Law (equation (1)) for the pore water electrical conductivity (ECw) under dry and wet marsh conditions. We then used the seawater equation of state to convert each ECw value to a salinity value. Subtracting the salinity values yielded the change in salinity required to account for the observed decrease in ECa between dry and wet marsh conditions. To reduce one excess degree of freedom in the calculation we assumed that these areas of the marsh remained water-saturated, leading to a minimum estimate of salinity change because the effect of any concurrent increase in soil water content would have reduced the magnitude of ΔECa. Field observations suggested that these areas of the marsh did remain

data sets. We represented marsh plain topography by a 2-m horizontal resolution kriged map of 742 marsh plain surface elevations surveyed using a total station, verified against LIDAR data. Major tidal channels are typically identified from aerial imagery, but we could find no precedent for mapping the small (0.1–0.5 cm wide by 0.1–0.5 cm deep) permanent drainage pathways hidden under the vegetation canopy that we term "microtributaries". We identified the thalwegs of microtributaries and banks of major tidal channels by traversing them with a streaming GPS (20-cm postprocessed horizontal accuracy). Two distance-to-channel metrics were calculated as the shortest straight-line distances from the center of each elevation grid cell to: (1) the nearest of the two primary tidal channels (bounding and bisecting the study area, Figure 2); (2) the nearest channel of any size.
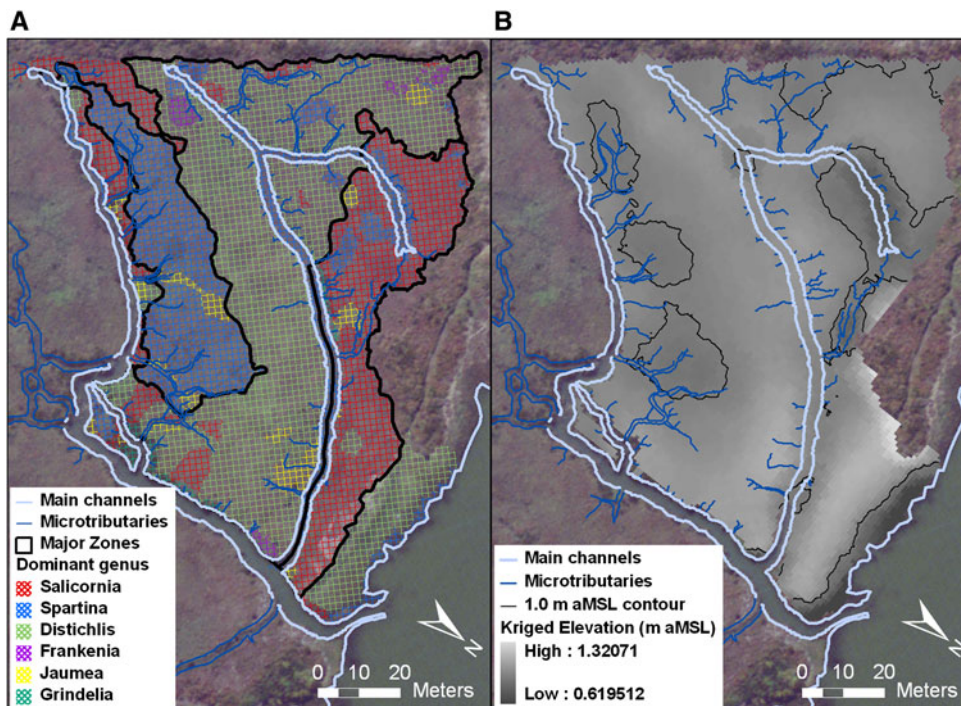
Figure 2. **A** Major vegetation zones, classified by the species of greatest cover fraction. **B** Site topography, units: meters above mean sea level.

Statistical Vegetation Differentiation

To contrast the utility of the six metrics described above in differentiating vegetation zones and plant species habitats, we employed binary logistic regression (BLR) models (SPSS 2009). A logistic regression is analogous to a linear regression but with a categorical, instead of continuous, dependent variable. By comparing the vegetation at each location in the marsh to the collocated values of the six metrics and repeating this for all marsh locations, the BLR method built models of those combinations of the six metrics that best distinguished the selected vegetation zone or habitat type. BLR models were assessed at the 95% confidence level.

We tested 108 BLR models, including univariate and multivariate analyses for each vegetation zone and species habitat. In the univariate cases we assessed whether any of the six metrics, alone, could correctly differentiate the marsh areas inside and outside each of the six major vegetation zones (6 metrics × 6 zones = 36 zone models). We also tested whether any of the six metrics, alone, could correctly differentiate the marsh areas occupied or not occupied by each species, regardless of its cover density (6 metrics × 6 species = 36 habitat models). These 72 models served to test the univariate predictive capacity of each of the six metrics in relation to vegetation patterning at our site. For these models, the two-fold null hypothesis in each case was either 100% or 0% cover by the selected zone or species.

In the multivariate analyses, we built forward-conditional BLR models for each vegetation zone and species habitat. This approach tested whether a combination of multiple metrics could better identify the distinguishing characteristics of each zone and habitat than a single metric. We tested three metric combinations: (1) the three geographic metrics, (2) the three edaphic metrics, (3) all six metrics, for a total of 36 multivariate models (3 combinations × (6 zones + 6 habitats) = 36 models). The forward-conditional BLR method selected only those metrics that significantly contributed to the zone or habitat prediction at the 95% confidence level. For these models, the two-fold null hypothesis in each case was either 100% or 0% cover by the selected zone or species. The results of the BLR models revealed the key characteristics distinguishing each plant habitat envelope and vegetation zone at our site.

RESULTS

Vegetation Patterns and Marsh Geometry

The spatial distribution of vegetation zones at the site is shown in Figure 2A, with zones labeled by the genus of the dominant species. Quadrat surveys verified that species identified as zone dominants occupied a majority (59% ± 16%) of the zone's cover. Zones dominated by the succulent *Salicornia* (28% of total marsh area) and the grasses *Spartina* (19%) and *Distichlis* (47%) were most prominent at

the site, with smaller areas dominated by *Jaumea* (4%), *Frankenia* (1%), and *Grindelia* (2%). *Salsola* and *Atriplex* individuals were present in only a few locations. The thick black outlines in Figure 2A highlight the three major vegetation zones, dominated by *Spartina*, *Distichlis*, and *Salicornia*. Zone assemblage compositions are illustrated by maps of relative cover density for each species (see supplement Figure S1), which were used to assess the total habitat occupied by each species.

The elevation ranges ($\mu \pm 1\sigma$ m above mean sea level) spanned by the species were not distinct: *Distichlis*, 1.04 ± 0.04; *Salicornia*, 1.03 ± 0.05; *Spartina*, 1.00 ± 0.06; *Jaumea*, 1.03 ± 0.05; *Frankenia*, 1.03 ± 0.03; *Grindelia*, 1.04 ± 0.03. Overlap between the elevation ranges of key species is common in salt marshes despite their characteristically distinct vegetation zonation (for example, Silvestri and others 2005; Sadro and others 2007). The average marsh plain elevation from the kriged topographic data was 1.02 ± 0.06 m above mean sea level (m aMSL) and ranged from 0.61 to 1.32 m. The seeming visual correlation between areas of slightly lower elevation and the southern, *Spartina*-dominated zone (Figure 2B) was not statistically supported because those same elevations elsewhere in the marsh were dominated by different species. Employed in univariate BLR models, elevation alone failed to justify rejecting the null hypothesis for any of the vegetation zones or species habitats at our site (Tables 1, 2, Model 1).

Qualitative assessment of marsh locations' distance to primary tidal channels showed the major zones dominated by *Spartina*, *Distichlis*, and *Salicornia* each occurred at any distance from the major tidal channels that bounded and bisected the marsh (Figure 3A). The *Spartina*-dominated zone appeared to coincide with a region of dense microtributaries (Figure 3B), yet neither distance-to-channel metric warranted rejecting the univariate BLR models' null hypothesis for any of the vegetation zones or species habitats (Tables 1, 2, Models 2, 3).

Edaphic Conditions and Vegetation

The spatial structure of edaphic conditions throughout the marsh, and the magnitude of ECa values reflecting these conditions, remained consistent between the dry (Figure 4A) and wet (Figure 4B) surveys. Mean ECa values for the two surveys were 13.37 and 13.71 dS/m, respectively (2.05 dS/m standard deviations; correlation coefficient $r = 0.83$). Despite their similarity, the ECa differences between wet and dry conditions were significant compared to the instrument accuracy (0.001 dS/m) and uncertainty (0.01 dS/m). Tensi-

ometer data confirmed that the root zone was drier during the first, "dry" geophysical survey than during the second, "wet" survey. Tides rapidly and uniformly covered the marsh to a depth of 0.5 m during spring tide flood events between the surveys. The specific relationships between ECa values and edaphic conditions (soil solution and paste extract conductivities and water and clay contents) determined for this salt marsh are presented in Table 3, which permit interpretation of the ECa data in terms of physical and chemical soil properties.

Despite the extreme environment, correlations between our ECa and soil core data showed that salt marsh ECa measurements can be interpreted in terms of three key edaphic properties: water content, salt content, and clay content. Variability in ECa values was significantly related to variability in each of these edaphic properties ($P < 0.005$, Table 3). At our site the EMI signal was dominated by the total salt content of the soil (as measured by the soil paste extract conductivity, ECe) but the volumetric soil water (θ) and clay content also contributed. See the online supplement for comparison of our salt marsh relationships with prior published relationships at lower water, salt, or clay contents. In brief, we conclude that the salt marsh ECa/ECe and ECa/θ relationships scale as in other environments but that the soil pore solution conductivity (ECw) and soil clay content of intertidal salt marshes have unique effects on EMI signals.

The configuration of vegetation zones (Figure 2A) did not resemble the spatial pattern of edaphic conditions (Figure 4). Instead, interior marsh areas that exhibited persistently high soil water content and/or salinity (high ECa) appeared coincident with major zone boundaries. A phenomenon of stressful edaphic conditions and major zone boundaries occurring in the same location was described for *Spartina* and *Salicornia* in northern San Francisco Bay salt marshes by Mahall and Park (1976) but had not been illustrated in plan view; our result is consistent with this explanation of ecotone locations. Though not consistently correlated with any vegetation zone or elevation, the edaphic conditions in the marsh at each point in time were significantly related to the hydrologic processes represented by the distance-to-channel metrics ($r = 0.36$ to 0.54). Low soil saturation, salinity, and/or clay content (low ECa) occurred close to tidal channels and more stressful edaphic conditions (high ECa) occurred further from the channels. Neither ECa data set provided information sufficient to reject the null hypothesis of the univariate BLR models (Tables 1, 2, Models 4, 5).

Table 1. Zone Discrimination by Zone-Specific Characteristics

F-C BLR zone models	Characteristic metrics	(a) Distichlis	(b) Salicornia	(c) Spartina	(d) Jaumea	(e) Frankenia	(f) Grindelia
1–5	Elevation OR dist. to major chan. OR dist. to any chan. OR dry ECa OR wet ECa	Null	Null	Null	Null	Null	Null
6	ΔECa	Null	*	*	*	*	*
	Correct in zone		44.4%	30.4%	31.8%	21.7%	33.3%
	Correct not in zone		66.9%	62.7%	63.9%	63.9%	64.0%
	Total correct		61.2%	56.4%	62.6%	63.4%	63.6%
7	Elevation	*	*	*	*	*	*
	Dist. to major chan.	*	*	*	–	–	*
	Dist. to any chan.	*	*	*	*	–	–
	Correct in zone	44.5%	Null	9.4%	Null	Null	Null
	Correct not in zone	71.5%		96.1%			
	Total correct	58.4%		79.2%			
8	Dry ECa	–	–	*	*	*	*
	Wet ECa	–	*	–	–	–	–
	ΔECa	–	*	–	–	–	–
	Correct in zone	Null	Null	Null	Null	Null	Null
	Correct not in zone						
	Total correct						
9	Elevation	*	*	–	–	*	*
	Dist. to major chan.	*	*	*	*	–	*
	Dist. to any chan.	*	*	*	–	–	–
	Dry ECa	–	*	*	*	–	*
	Wet ECa	–	–	–	–	–	–
	ΔECa	*	–	–	–	–	–
	Correct in zone	46.7%	Null	12.7%	Null	Null	Null
	Correct not in zone	68.1%		96.5%			
	Total correct	57.7%		80.2%			

The two-fold null hypothesis for each model was either 0% or 100% cover by the selected zone or species.
*Significant contributor to the model at the 95% confidence level.
–Removed from the model by the forward-conditional process.
The table is read as in the following examples. BLR Model 6(b) tested how well the ΔECa metric differentiated areas inside and outside the Salicornia-dominated zone. ΔECa contributed significantly to the model prediction. The model correctly identified 44.4% of the areas mapped inside a Salicornia-dominated zone and 66.9% of the areas mapped outside a Salicornia-dominated zone. In all, the model correctly predicted 61.2% of the marsh area with respect to its status as Salicornia-dominated or not. In contrast, BLR Model 6(a) tested how well the ΔECa metric differentiated areas inside and outside the Distichlis-dominated zone. This model was unable to leverage the information contained in the ΔECa metric to differentiate areas of the marsh dominated or not dominated by Distichlis, resulting in the model assigning the entire marsh to a single category, equivalent to the null hypothesis.
The zone-oriented BLR models tested whether six metrics, alone (models 1–6) or in combination (models 7–9), could correctly differentiate the vegetation zones at the site (see Figure 2A).

The spatial pattern of tidally induced changes in edaphic conditions, revealed by subtracting the wet and dry ECa surveys (ΔECa, Figure 5A), was more heterogeneous than the spatial variability in static edaphic conditions (Figure 4). The pattern of change was not altered by the Q-DEMI calculations, which converted ΔECa values to soil saturation and salinity change quantities (Figure 5B). The conversion was made using values of f = 0.223 and σ_s = 2.479 dS/m. The average estimated saturation change in the fluid-exchange dominated areas of the marsh (blue in Figure 5B) was 6.2 ± 5.5% ($\mu \pm 1\sigma$). The average estimated salt loss from the salt-exchange dominated areas of the marsh (red in Figure 5B) was 0.77 ± 0.64 kg/m². The large standard deviations of these average results were due to highly spatially heterogeneous soil aeration and flushing throughout the marsh, not due to measurement uncertainty or error. Despite the Q-DEMI methodology producing conservative estimates of the magnitude of edaphic change, we emphasize that the methodology permits expedient

Table 2.   Habitat Discrimination by Species-Specific Characteristics

F-C BLR habitat models	Characteristic metrics	(a) Distichlis	(b) Salicornia	(c) Spartina	(d) Jaumea	(e) Frankenia	(f) Grindelia
1–5	Elevation OR dist. to major chan. OR dist. to any chan. OR dry ECa OR wet ECa	Null	Null	Null	Null	Null	Null
6	ΔECa	*	*	*	*	*	*
	Correct present	64.3%	64.3%	69.5%	73.0%	27.9%	22.8%
	Correct absent	36.5%	44.3%	41.1%	45.7%	63.4%	60.1%
	Total correct	54.8%	63.7%	54.8%	59.9%	60.6%	51.5%
7	Elevation	*	*	–	–	*	–
	Dist. to major chan.	*	*	*	*	–	*
	Dist. to any chan.	*	*	*	*	–	–
	Correct present	93.0%	Null	50.2%	58.0%	Null	Null
	Correct absent	12.3%		75.0%	55.8%		
	Total correct	65.4%		63.0%	57.0%		
8	Dry ECa	*	–	–	–	*	*
	Wet ECa	–	*	*	–	–	–
	ΔECa	–	–	*	*	–	*
	Correct present	Null	Null	44.2%	73.0%	Null	Null
	Correct absent			68.2%	45.7%		
	Total correct			56.6%	59.9%		
9	Elevation	*	*	–	–	*	–
	Dist. to major chan.	*	*	*	–	–	*
	Dist. to any chan.	*	–	*	–	–	–
	Dry ECa	*	–	–	–	–	–
	Wet ECa	–	*	–	–	–	–
	ΔECa	–	–	*	*	*	*
	Correct present	92.2%	Null	58.8%	73.0%	Null	19.6%
	Correct absent	13.8%		70.1%	45.7%		95.9%
	Total correct	65.4%		64.6%	59.9%		78.4%

The two-fold null hypothesis for each model was either 0% or 100% cover by the selected zone or species.
*Significant contributor to the model at the 95% confidence level.
–Removed from the model by the forward-conditional process.
The habitat-oriented BLR models tested whether six metrics, alone or in combination, could correctly differentiate the marsh areas occupied or not occupied by each species, regardless of its cover density (see supplement Figure S1). The table is read in the same manner as Table 1.

mapping of the magnitude of salt and water exchange in a spatially distributed way throughout a salt marsh.

Spatial patterns of saturation and salinity change did not qualitatively resemble vegetation zonation (Figures 2A, 5B), yet BLR models based on ΔECa were able to partially describe the zones dominated by every species except *Distichlis*. For the *Salicornia*-, *Spartina*-, *Jaumea*-, *Frankenia*-, and *Grindelia*-dominated zones, the BLR models correctly distinguished 22–44% of the area inside each zone and 63–67% of the area outside each zone (Table 1, Model 6). Although short of the ideal prediction (100% correct both inside and outside each zone),

these results using the ΔECa metric were a substantial improvement (with 95% confidence) over the null hypothesis returned by the BLR models based on the other five metrics.

ΔECa BLR models were more successful at distinguishing between marsh areas occupied and not occupied by each of the six plant species, regardless of cover density (supplement Figure S1), compared to distinguishing between vegetation zones. ΔECa BLR habitat models (Table 2, Model 6) correctly identified 64% of the observed *Distichlis* and *Salicornia* occurrences and 37% and 44% of observed absences, respectively. ΔECa BLR models for *Spartina* and *Jaumea* habitat correctly predicted 70%
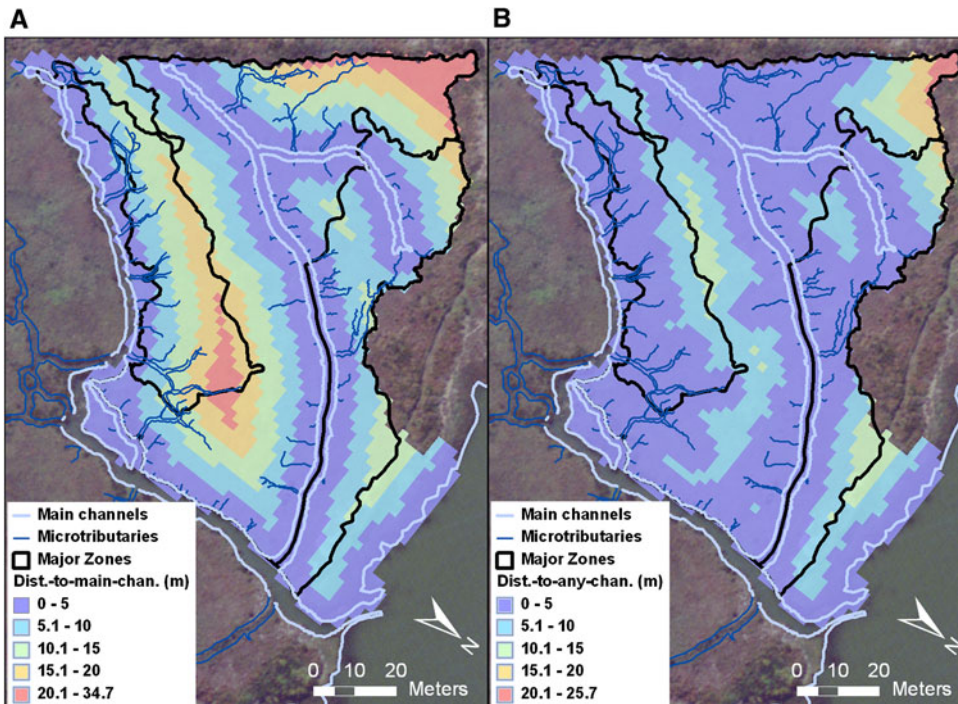
Figure 3. A Shortest distance to one of the main tidal channels, shown in *light blue* bounding and bisecting the marsh site. **B** Shortest distance to the nearest channel of any size, including microtributaries shown in *dark blue*.
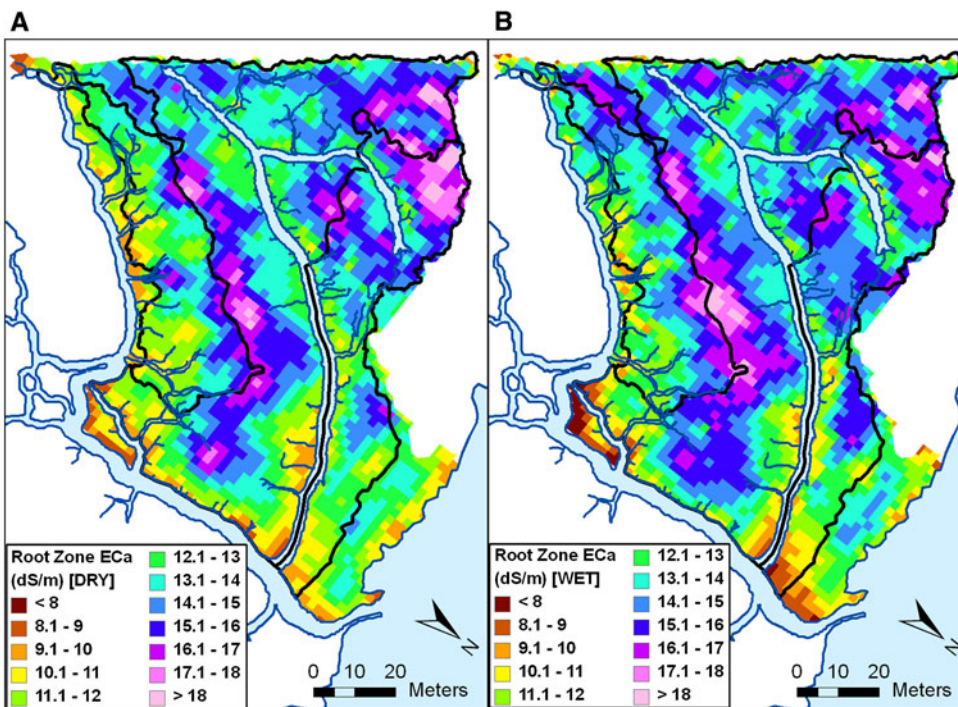

Figure 4. Root zone bulk soil electrical conductivity (ECa) from (**A**) dry and (**B**) wet marsh conditions. *Dark blue* lines are channel and microtributary banks, *black* lines depict major vegetation zone boundaries.

and 73% of the observed occurrences and 41% and 46% of observed absences, respectively. ΔECa BLR models for *Frankenia* and *Grindelia* were less successful at correctly predicting occurrences of these species (28% and 23%, respectively) but more successful at correctly predicting absences (63% and 60%, respectively). For all six species, the ΔECa BLR habitat models justified rejecting the null hypotheses (with 95% confidence).

The patterns in edaphic conditions and geographic metrics of salt marsh structure supported our two hypotheses regarding the spatial nature of zonation-relevant variables and their relationship to salt marsh vegetation distribution:

(1) Multiple metrics relevant to salt marsh vegetation zonation each exhibit different patterns. These patterns are characterized by different

Table 3. Relation of ECa Data to Soil Properties

Property	Sample statistics		Correlation with ECa
	Mean	Standard deviation	
Soil paste extract electrical conductivity[1] (ECe, dS/m)	68.9	15.0	0.67
Soil pore water electrical conductivity[2] (ECw, dS/m)	57.2	7.0	0.53
Soil volumetric water content[1] (θ)	0.83	0.15	0.43
Soil clay content[1] (%)	61.8	9.4	0.51
Soil temperature[3] (dry conditions, °C)	13.98	0.54	–
Soil temperature[3] (wet conditions, °C)	11.56	0.41	–
Tide water electrical conductivity (EC$_{tide}$, dS/m)	33.4	–	–

[1]N = 23.
[2]N = 17.
[3]N = 14.
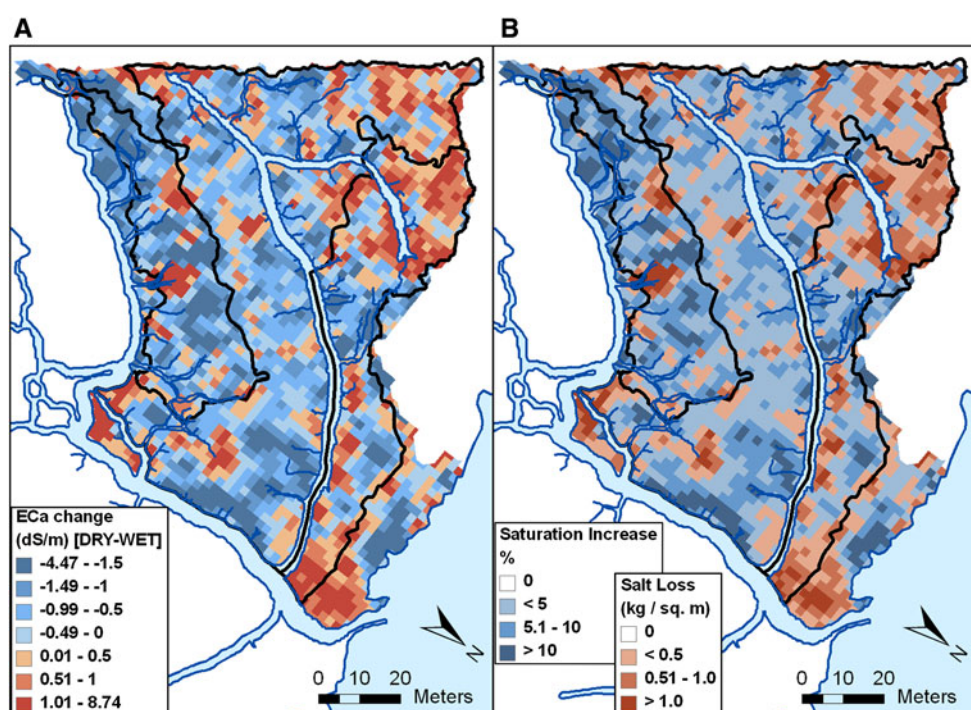
Figure 5. **A** Edaphic change between dry and wet marsh conditions, represented by the change in bulk soil electrical conductivity (ΔECa, dS/m). **B** Result of Q-DEMI conversion of ΔECa to changes in root zone saturation (%) or salinity (kg/m^2) between dry and wet marsh conditions. *Blue areas* were dominated by net saturation increase between dry and wet conditions, *red* areas were dominated by net salinity decrease. *Dark blue* lines are channel and microtributary banks, *black lines* depict major vegetation zone boundaries.

spatial scales and degrees of spatial heterogeneity. Alone, only the ΔECa metric provided information useful in indentifying vegetation zones and species habitats.

(2) The relation of ΔECa to vegetation distribution differed depending on the species considered and whether the species was considered alone or as a zone-dominant.

Multivariate Vegetation Zone and Habitat Discrimination

We conjectured that a combination of multiple metrics might better discriminate salt marsh vegetation zones and individual species habitats than univariate models. The metric combinations we tested using forward-conditional BLR models were: (1) the three geographic metrics, (2) the three edaphic metrics, and (3) all six metrics. Salient results are presented here; complete BLR model results are provided in Tables 1 and 2.

Except in the case of the *Distichlis*-dominated zone, none of the multivariate models identified vegetation zones or habitats considerably better than the univariate ΔECa BLR models. For the *Distichlis*-dominated zone, a BLR model including all three geographic metrics correctly predicted 45% of the marsh area within the zone and 72% of the area outside the zone (Table 1, Model 7(a)), compared to the null hypothesis returned by

the univariate ΔECa BLR model. In contrast, the dominance of the other five major species at the site may be more related to the magnitude of temporal variation in root zone soil water content and soil salinity, represented by the ΔECa metric, than geographic effects. For example, ΔECa was the *only* significant predictor of the marsh areas that *Jaumea* occupied, even when the other five metrics were made available to the forward-conditional model. However, a BLR model based on ΔECa correctly predicted 73% of *Jaumea* occurrences in the salt marsh (Table 2, Models 6(d), 9(d)) but only 32% of *Jaumea*-dominated zone area (Table 1, Model 6(d)).

DISCUSSION

Spatial Variability in Edaphic Conditions

Unexpectedly poor spatial correlation between edaphic conditions (represented by ECa data from one point in time) and proxies for hydrologic forcing (elevation and distance-to-channel metrics) suggests that spatial patterns of tide-induced edaphic change were not dominantly hydrologic in origin. The spatial patterns of the ECa measurements must naturally vary in accord with those variables that permit the conduction of electricity through the subsurface: soil saturation, salinity, and clay content (Friedman 2005; Rhoades and others 1999). Soil temperature also affects the magnitude of ECa measurements (Reedy and Scanlon 2003). The similarity of the overall spatial patterns of ECa between wet and dry marsh conditions suggested that those component factors contributing most strongly to the ECa signal were roughly constant in time.

Despite only slight variation in the generally clayey soil texture recovered by our soil samples, small spatial variations in soil texture, static in time, likely contributed to the observed spatial pattern of ECa. As a confounding factor, however, both salt and water exhibit great affinity for clay soils and will be displaced by diffusion or advection only in small measure under small natural gradients. At our site, the correlations between the clay content and water content ($r^2 = 0.03$) or pore water salinity ($r^2 = 0.04$) of our soil samples were weak but the correlation between clay content and interstitial, non-aqueous soil salinity was strong ($r^2 = 0.49$; see IECI in online supplement). In combination with evidence from the correlation of the soil core properties with collocated ECa measurements (supplement, Figure S2), this suggested

that the pattern of ECa values from one point in time (wet or dry conditions) was likely most strongly influenced by soil texture and non-aqueous soil salinity. In this light, the poor correlation between ECa values and proxies for hydrologic forcing was less of a mystery as hydrologic dynamics were most likely to influence soil water content and aqueous soil salinity over short time scales, not the soil texture and interstitial soil salinity contributing the most to the ECa measurements. This analysis is consistent with model results indicating that different values of soil hydraulic conductivity affect the magnitude, but not the location, of salt marsh soil salinity (Wang and others 2007).

Although we base our interpretation of the geophysical data on logical deduction and ancillary data from soil cores, pore water samples, and tidal and groundwater monitoring, the determination of non-geophysical insight from geophysical data is a complex process (Robinson and others 2008b). Potential sources of uncertainty in our data include unaccounted-for spatial variation in ground temperature and small ponds of surface water hidden beneath matted vegetation. Another source of uncertainty regarding the interpretation of ECa in terms of soil properties was the discrepancy between the estimated depth interval supporting the ECa measurements (0–40 cm) and the depth interval of the correlated core samples (0–30 cm). The discrepancy arose because the 0–30 cm soil core depth had to be chosen a priori because the 0–40 cm soil depth interval represented by the ECa data could only be estimated after ECa data collection (see supplement). The sensitivity of the ECa instrument is greatest at shallower depths within the measured sediment profile (Abdu and others 2007), so the localized presence of different conditions in the 30–40 cm depth layer would only slightly perturb the ECa measurements. In this study, such uncertainty was further reduced because the core samples obtained from the 30–60 cm depth interval were very similar to those from the 0–30 cm depth interval. Lastly, this uncertainty regarding the interpretation of ECa in terms of soil properties did not affect our interpretation of the relationship between the ECa or ΔECa geophysical data and the vegetation patterns. We constrained the parameters used in the Q-DEMI calculations by comparing multiple parameter estimation methods, but the parameters remain estimates of petrophysical relationships and as such are uncertain, although reasonable for the soils analyzed in this study (see supplement).

Tide-Induced Edaphic Change and Vegetation Zonation

Although the logistic regression models identified, in most cases, major characteristics that distinguished the vegetation zones and species habitats at our site, a striking result was that some zones and species habitats were identified by a combination of multiple variables (for example, *Distichlis*) but others were best identified by a single variable (for example, *Jaumea*). There was also a surprisingly large difference in the ability of the models to describe the key characteristics of the total habitat envelope of a species versus the zone for which it provided the dominant cover class: the regression models were generally better able to identify characteristic individual plant species habitats than vegetation zones. In most cases, the ΔECa metric, alone, was most useful for identifying vegetation zones and species habitats. The Q-DEMI method and soil core analyses showed that ΔECa represented the amount of water and salt exchanged from the root zone between two points in time. The data from this study could not definitively separate, however, whether observed changes in edaphic conditions were due entirely to intervening tidal flooding, or due to the interaction of hydrologic forcing with spatial variability in factors such as soil density, root holes, and bioturbation, and plant water and salt uptake. The lack of correlation between ΔECa and either elevation or distance-to-channel argues against the hydrologic processes implied by the elevation and distance-to-channel metrics as the dominant determinants of spatial patterns in edaphic change.

Intertidal salt marsh soil water content and salinity change significantly over the short spring/neap tidal cycle time scale in response to tidal influences, as revealed by this study. Over similar time scales, gradual changes to marsh topography, channel geometry, and vegetation patterning are negligible. Continued observations of field conditions over more than 3 years (2006–2010) suggested stable topography, channels, and vegetation zonation at the field site, consistent with the temporal "snapshots" analyzed in this study. Over longer time scales, geomorphological processes may alter marsh surface microtopography and vegetation zones may shift somewhat due to disturbance and interspecific interactions (for example, Byrd and Kelly 2006). Other environmental factors that may affect vegetation zonation in salt marshes that were not examined in this study include nutrient availability, herbivory, and site history. Once drainage is established and a marsh plain vegetated,

the time scale of salt marsh tidal channel network geometry change is decadal to millennial (Allen 2000), barring substantial changes in tidal regime or sea level (for example, Kirwan and Murray 2007). Some marsh sites may retain such stable vegetation patterns for hundreds of years (for example, Orson and Howes 1992; Allen 2000; Schwimmer and Pizzuto 2000), although catastrophic disturbance may rapidly shift a marsh into a different regime (van de Koppel and others 2005; Kirwan and others 2008). The lack of correlation between vegetation zonation and elevation or distance-to-channel in this case study of a mature salt marsh argues for increased consideration of shorter-term environmental effects. Hence, the focus of this study was on the relationships between vegetation and soil conditions, within the context of a given salt marsh regime of specified vegetation and tidal channel geometry.

The phenomenon of large, broadly distributed decreases in soil salinity, identified in this study by decreases in ECa between dry and wet marsh conditions, has not previously been reported and the precise cause is unknown. Potential mechanisms for what was apparently rapid flood tide-induced salt removal from the salt marsh root zone include: diffusion, leaching, or dissolution of salt from the surface; plant salt uptake; or dilution by convective mixing in soil macropores. The simplest of these hypothetical mechanisms of salt loss is the dilution of evapoconcentrated pore water by mixing with less saline tidal surface water. Yet, it is unlikely that dilution alone can fully account for the observed decreases in marsh soil salinity between dry and wet marsh conditions. On average, the 0.77 kg/m^2 of salt loss from the salt-exchange dominated areas of the marsh accounted for approximately 15% of the root zone pore fluid salinity. To achieve 15% dilution of the root zone pore fluids in these areas, the less saline tidal surface waters would have to have infiltrated about 70% of the root zone. Even if the stratification of less saline tidal water over more saline marsh pore water were overcome and mixing occurred, it is physically unlikely that seven-tenths of the pore space in the fine-textured, largely saturated marsh root zone would be flushed by surface water during the short duration of a flooding tide. It is most likely that multiple mechanisms of salt exchange between the marsh surface and tidal waters operate simultaneously. For example, salt uptake by vegetation could account for some of the observed salinity decrease and reduce the amount of pore water turn-over required to account for the observations.

Conclusion

The effects of root zone salinity, water content, and soil texture on salt marsh vegetation zonation are implicitly combined in nature. The combination of spatially variable root zone salinity, water content, and soil texture is also represented in EMI measurements of bulk apparent soil electrical conductivity (ECa). Although the relationships between edaphic factors and ECa data and between edaphic factors and vegetation zonation are surely different, this study demonstrated the potential of EMI technology to expose emergent spatial and temporal edaphic patterns and properties that are more than the sum of the contributing variables. Multiple contributing variables logically affect the distribution of interacting species assemblages differently than the distribution of individuals, but multivariate relationships between abiotic and biotic ecosystem patterns are difficult to assess without high-resolution spatially distributed data. Though linkages between edaphic conditions and vegetation zonation can only be established in a correlative manner with these and prior such surveying methods (for example, Vince and Snow 1984), geophysical methods such as EMI and Q-DEMI provide means to obtain high-resolution, spatially distributed data on root zone soil properties that have previously been prohibitively difficult to obtain over broad areas. In this study, such edaphic data were more useful in characterizing salt marsh vegetation zones and habitats than traditional geographic metrics such as elevation and distance-to-channel.

The challenge of predicting the vegetation distribution of intertidal salt marsh ecosystems persists. Despite functional similarity between different salt marsh species around the world, regional and latitudinal differences so far prohibit development of a universally applicable, mechanistic, zonation model (Farina and others 2009; Pennings and others 2003). Even if such a model was possible, its accuracy would necessarily vary from site to site. Some of the most pressing questions regarding salt marsh vegetation zonation, such as the expected response of a marsh to restoration efforts or to an invasive species, must be answered on a site-by-site basis and may require probabilistic, not deterministic, answers. Site mapping, EMI geophysics, and the Q-DEMI methodology can provide a cost-effective, rapid, and repeatable means to statistically characterize a salt marsh site. The resulting spatial and temporal patterns might then be used as a foundation upon which to interpret or predict vegetation distributions and biotic interactions based on existing region- and species-specific knowledge. Linking plot-scale studies of plant–soil relations and interspecific interactions to marsh-scale studies of spatial variability provides a promising means to fill the gap between the general principles and site-specific needs of salt marsh vegetation zonation science and restoration.

Supplementary Information

Further supplementary information is provided online, containing details on: complete vegetation maps, EMI signal depth calculation, ECa uncertainty determination, soil sampling results and ECa relationship to edaphic conditions, Archie's Law parameter estimations: f, φ, and σ_s, and cross-correlation of geographic and edaphic metrics.

REFERENCES

Abdu H, Robinson DA, Jones SB. 2007. Comparing bulk soil electrical conductivity determination using the DUALEM-1S and EM38-DD electromagnetic induction instruments. Soil Sci Soc Am J 71:189–96.

Allen JRL. 2000. Morphodynamics of Holocene salt marshes: a review sketch from the Atlantic and Southern North Sea coasts of Europe. Q Sci Rev 19:1155–231.

Bertness MD, Gough L, Shumway SW. 1992. Salt tolerances and the distribution of fugitive salt marsh plants. Ecology 73:1842–51.

Byrd KB, Kelly M. 2006. Salt marsh vegetation response to edaphic and topographic changes from upland sedimentation in a Pacific estuary. Wetlands 26:813–29.

Cooper WS. 1926. Vegetational development upon alluvial fans in the vicinity of Palo Alto, California. Ecology 6:325–473.

Corwin DL, Lesch SM. 2005. Applications of apparent soil electrical conductivity in precision agriculture. Comput Electron Agric 46:103–33.

Emery NC, Ewanchuk PJ, Bertness MD. 2001. Competition and salt-marsh plant zonation: stress tolerators may be dominant competitors. Ecology 82:2471–85.

Farina JM, Silliman BR, Bertness MD. 2009. Can conservation biologists rely on established community structure rules to manage novel systems? … Not in salt marshes. Ecol Appl 19(2):413–22.

Freeze RA, Cherry JA. 1979. Groundwater. Upper Saddle River: Prentice Hall.

Friedman SP. 2005. Soil properties influencing apparent electrical conductivity: a review. Comput Electron Agric 46:45–7.

Hamlin SN. 1983. Injection of treated wastewater for groundwater recharge in the Palo Alto Baylands, California: Hydraulic and chemical interactions—preliminary report. U.S. Geological Survey Water-Resources Investigation Report 82-4121.

Hinde HP. 1954. The vertical distribution of salt marsh phanerogams in relation to tide levels. Ecol Monogr 24:209–25.

Kirsch R. 2006. Petrophysical properties of permeable and low-permeable rocks. In: Kirsch R, Ed. Groundwater geophysics. New York: Springer.

Kirwan ML, Murray AB. 2007. A coupled geomorphic and ecological model of tidal marsh evolution. Proc Natl Acad Sci USA 104:6118–22.

Kirwan ML, Murray AB, Boyd WS. 2008. Temporary vegetation disturbance as an explanation for permanent loss of tidal wetlands. Geophys Res Lett 35:L05403.

Lesch SM. 2005. Sensor directed response surface sampling designs for characterizing variation in soil properties. Comput Electron Agric 46:153–79.

Lesch SM, Corwin DL, Robinson DA. 2005. Apparent soil electrical conductivity mapping as an agricultural management tool in arid zone soils. Comput Electron Agric 46:351–78.

Mahall BE, Park RB. 1976. The ecotone between *Spartina foliosa* trin. and *Salicornia virginica* l. in salt marshes of northern San Francisco Bay: I. biomass and production. J Ecol 64:421–33.

Marani M, Silvestri S, Belluco E, Ursino N, Comerlati A, Tosatto O, Putti M. 2006. Spatial organization and ecohydrological interactions in oxygen-limited vegetation ecosystems. Water Resour Res 42:W06D06.

Orson RA, Howes BL. 1992. Salt marsh development studies at Waquoit Bay, Massachusetts: influence of geomorphology on long-term plant community structure. Estuar Coast Shelf Sci 35:453–71.

Paine JG, White WA, Smyth RC, Andrews JR, Gibeaut JC. 2004. Mapping coastal environments with lidar and EM on Mustang Island, Texas, U.S. Lead Edge 23:894–8.

Pennings SC, Callaway RM. 1992. Salt marsh plant zonation: the relative importance of competition and physical factors. Ecology 73:681–90.

Pennings SC, Selig ER, Houser LT, Bertness MD. 2003. Geographic variation in positive and negative interactions among salt marsh plants. Ecology 84(6):1527–38.

Pennings SC, Grant M-B, Bertness MD. 2005. Plant zonation in low-latitude salt marshes: disentangling the roles of flooding, salinity and competition. J Ecol 93:159–67.

Peterson CH, Able KW, DeJong CF, Piehler MF, Simenstad CA, Zedler JB. 2008. Practical proxies for tidal marsh ecosystem services: application to injury and restoration. Adv Mar Biol 54:221–66.

Reedy RC, Scanlon BR. 2003. Soil water content monitoring using electromagnetic induction. J Geotech Geoenvironmental Eng 129:1028–39.

Rhoades JD, Chanduvi F, Lesch S. 1999. Soil salinity assessment: methods and interpretation of electrical conductivity measurements. Irrigation and Drainage Paper 57, FAO, Rome, Italy.

Robinson DA, Abdu H, Jones SB, Seyfried M, Lebron I, Knight R. 2008a. Eco-geophysical imaging of watershed-scale soil patterns links with plant community spatial patterns. Vadose Zone J 7(4):1132–8.

Robinson DA, Binley A, Crook N, Day-Lewis FD, Ferré TPA, Grauch VJS, Knight R, Knoll M, Lakshmi V, Miller R, Nyquist J, Pellerin L, Singha K, Slater L. 2008b. Advancing process-based watershed hydrological research using near-surface geophysics: a vision for, and review of, electrical and magnetic geophysical methods. Hydrol Process 22:3604–35.

Robinson DA, Lebron I, Kocar B, Phan K, Sampson M, Crook N, Fendorf S. 2009. Time-lapse geophysical imaging of soil moisture dynamics in tropical deltaic soils: an aid to interpreting hydrological and geochemical processes. Water Resour Res 45:W00D32.

Roman CT, James-Pirri MJ, Heltshe JF. 2001. Monitoring salt marsh vegetation. National Park Service Inventory and Monitoring Protocol, Cape Cod. http://science.nature.nps.gov/im/monitor/protocols/caco_marshveg.pdf.

Sadro S, Gastil-Buhl M, Melack J. 2007. Characterizing patterns of plant distribution in a southern California salt marsh using remotely sensed topographic and hyperspectral data and local tidal fluctuations. Remote Sens Environ 110:226–39.

Sanderson EW, Foin TC, Ustin SL. 2001. A simple empirical model of salt marsh plant spatial distributions with respect to a tidal channel network. Ecol Model 139:293–307.

Scanlon BR, Paine JG, Goldsmith RS. 1999. Evaluation of electromagnetic induction as a reconnaissance technique to characterize unsaturated flow in an arid setting. Ground Water 37:296–304.

Schwimmer RA, Pizzuto JE. 2000. A model for the evolution of marsh shorelines. J Sed Res 70:1026–35.

Silvestri S, Defina A, Marani M. 2005. Tidal regime, salinity and salt marsh plant zonation. Estuar Coast Shelf Sci 62:119–30.

SPSS. 2009. PASW statistics 17. Chicago (IL): SPSS Inc.

Stroh JC, Archer S, Doolittle JA, Wilding L. 2001. Detection of edaphic discontinuities with ground-penetrating radar and electromagnetic induction. Landsc Ecol 16:377–90.

Turner MG, Chapin FSIII. 2005. Causes and consequences of spatial heterogeneity in ecosystem function. In: Lovett GM, Jones CG, Turner MG, Weathers KC, Eds. Ecosystem function in heterogeneous landscapes. New York: Springer.

USDA. 2009. Plants Database. U.S. Department of Agriculture, Natural Resources Conservation Service. http://plants.usda.gov/index.html

USFW. 2008. Species Account: California Clapper Rail. Species Account: Salt Marsh Harvest Mouse. U.S. Fish and Wildlife Service, Sacramento Office. http://www.fws.gov/sacramento/es/animal_spp_acct/

van de Koppel J, van der Wal D, Bakker JP, Herman PMJ. 2005. Self-organization and vegetation collapse in salt marsh ecosystems. Am Nat 165:E1–12. doi:10.1086/426602.

Vince SW, Snow AA. 1984. Plant zonation in an Alaskan salt marsh: I. Distribution, abundance, and environmental factors. J Ecol 72:651–67.

Wang H, Hsieh YP, Harwell MA, Huang W. 2007. Modeling soil salinity distribution along topographic gradients in tidal salt marshes in Atlantic and Gulf coast regions. Ecol Model 201:429–39.

Zedler JB, Callaway JC, Desmond JS, Vivian-Smith G, Williams GD, Sullivan G, Brewster AE, Bradshaw BK. 1999. Californian salt-marsh vegetation: an improved model of spatial pattern. Ecosystems 2:19–35.